Fluctuation and dissipation dynamics in fusion reactions from a stochastic mean-field approach

Sakir Ayik,[1] Kouhei Washiyama,[2] and Denis Lacroix[2]
[1]*Physics Department, Tennessee Technological University, Cookeville, Tennessee 38505, USA*
[2]*GANIL, Bd Henri Becquerel, BP 55027, F-14076 Caen Cedex 5, France*
(Received 3 February 2009; published 8 May 2009)

By projecting the stochastic mean-field dynamics on a suitable collective path during the entrance channel of heavy-ion collisions, expressions for transport coefficients associated with relative distance are extracted. These transport coefficients, which have forms similar to those familiar from the nucleon exchange model, are evaluated by carrying out time-dependent Hartree-Fock simulations. The calculations provide an accurate description of the magnitude and form factor of transport coefficients associated with one-body dissipation and fluctuation mechanisms.

DOI: 10.1103/PhysRevC.79.054606 PACS number(s): 25.70.Jj, 21.60.Jz, 24.60.Ky

I. INTRODUCTION

The self-consistent mean-field theory, also known as time-dependent Hartree-Fock (TDHF), by employing Skyrme-type effective interactions, has been extensively applied to describe nuclear collision dynamics at low bombarding energies below 10 MeV per nucleon [1–4]. In the mean-field theory, short-range two-body correlations are neglected and nucleons move in the self-consistent potential produced by all other nucleons. This is a good approximation at low energies because Pauli blocking is very effective for scattering into unoccupied states. Consequently, in the mean-field theory, collective energy is converted into intrinsic degrees of freedom via interaction of nucleons with the self-consistent mean-field, so-called one-body dissipation [5,6]. The one-body dissipation mechanism plays a dominant role in low energy nuclear dynamics including deep-inelastic heavy-ion collisions and heavy-ion fusion reactions. One important limitation of the mean-field theory is related to dynamical fluctuations of collective motion. In the mean-field description, while single-particle motion is treated in a quantal framework, collective motion is treated almost in a classical approximation. Therefore, TDHF provides a good description for average evolution; however, it severely underestimates fluctuations of collective variables.

However, it is well known that no dissipation takes place without fluctuations [7,8]. Much effort has been made to improve the one-body transport description beyond the mean-field. Most of these transport descriptions take into account dissipation and fluctuation mechanisms due to two-body collisions, which play an important role in nuclear dynamics at intermediate energies [9–12]. Here, we deal with nuclear dynamics at low energies at which one-body dissipation and associated mean-field fluctuations play a dominant role in dynamical evolution. One of the fundamental questions is how to improve the mean-field theory by incorporating the one-body fluctuation mechanism at a microscopic level? In a recent work, based on an appealing idea of Dasso [13] and Dasso and Donangelo [14], this question has been addressed. A stochastic mean-field (SMF) approach has been proposed for describing fluctuation dynamics [15,16]. For small amplitude fluctuations, this model gives a result for the dispersion of a one-body observable that is identical to the result obtained through a variational approach [17]. It is also shown that, when the SMF is projected on a collective variable, it gives rise to a generalized Langevin equation [18], which incorporates one-body dissipation and one-body fluctuation mechanisms in accordance with the quantal dissipation-fluctuation relation. These illustrations give strong support for the contention that the SMF approach provides a consistent microscopic description for the dynamics of density fluctuations in low energy nuclear reactions. In this article, we present another demonstration of the SMF approach.

In a recent work, by a suitable definition of collective variables of relative motion, the nucleus-nucleus potential energy and one-body friction coefficient as a function of relative distance have been extracted from simulations of microscopic TDHF [19] (see also Ref. [20]). Such a reduction is not constrained by adiabatic or diabatic approximation; therefore, it should provide an accurate description of conservative nucleus-nucleus potential energy and the magnitude of the one-body dissipation mechanism [21]. It is of great interest to deduce the magnitude of diffusion coefficients associated with collective variables. However, this information is not contained in the standard mean-field approximation. The SMF approach provides a proper framework for extracting dissipation and fluctuation properties of collective variables. In this work, we carry out a similar macroscopic reduction of the SMF approach on a collective path. In this manner, we deduce not only nucleus-nucleus potential and one-body friction coefficients, but also one-body diffusion coefficients associated with collective variables.

In Sec. II, we give a brief description of the SMF approach. In Sec. III, we present a suitable definition of collective variables in heavy-ion collisions and the correlation function of the Wigner distribution. In Sec. IV, we derive transport coefficients associated with relative motion from the SMF approach. In Sec. V, conclusions are given.

II. STOCHASTIC MEAN-FIELD APPROACH

In the standard TDHF, temporal evolution of the system is described by a single Slater determinant constructed with time-dependent single-particle wave functions, $\Phi_{j\sigma\tau}(\boldsymbol{r}, t)$.

The evolution of single-particle wave functions is determined by TDHF equations with proper initial conditions,

$$i\hbar\frac{\partial}{\partial t}\Phi_{j\sigma\tau}(\boldsymbol{r},t)=h(\rho)\Phi_{j\sigma\tau}(\boldsymbol{r},t), \tag{1}$$

where $h(\rho)$ denotes the self-consistent mean-field Hamiltonian with the one-body density ρ. For clarity of notation spin-isospin quantum numbers $\tau=$ (proton, neutron) and $\sigma=$ (spin-up, spin-down) are explicitly indicated in these expressions. In many situations, it is more appropriate to express the mean-field approximation in terms of the single-particle density matrix,

$$\rho(\boldsymbol{r},\boldsymbol{r}',t)=\sum_{j\sigma\tau}\Phi^{*}_{j\sigma\tau}(\boldsymbol{r},t)n_j^{\sigma\tau}\Phi_{j\sigma\tau}(\boldsymbol{r}',t), \tag{2}$$

where $n_j^{\sigma\tau}$ denotes occupation factors of single-particle states. In the standard TDHF, occupation factors are one and zero for the occupied and unoccupied states, respectively. If the initial state is at a finite temperature, the average occupation factors are determined by the Fermi-Dirac distribution.

TDHF provides a deterministic evolution of the single-particle density matrix, starting from a well-defined initial state and leading to a well-defined final state. To incorporate fluctuation mechanism into dynamics, we give up standard description in terms of a single Slater determinant and consider a superposition of determinantal wave functions. As a result of correlations, initial density cannot have a deterministic shape, but it must exhibit quantal zero-point fluctuations, and if the initial state is at a finite temperature, it also involves thermal fluctuations. In the SMF approach the initial density fluctuations are incorporated into the description in a stochastic manner [15]. The initial density fluctuations are simulated by representing the initial state in terms of a suitable ensemble. In this manner, an ensemble of density matrices is generated,

$$\rho^{\lambda}(\boldsymbol{r},\boldsymbol{r}',t)=\sum_{ij\sigma\tau}\Phi^{*}_{i\sigma\tau}(\boldsymbol{r},t;\lambda)\rho^{\lambda}_{ij}(\sigma\tau)\Phi_{j\sigma\tau}(\boldsymbol{r}',t;\lambda). \tag{3}$$

Here $\Phi_{j\sigma\tau}(\boldsymbol{r},t;\lambda)$ is a complete set of single-particle basis, λ denotes a member in the ensemble, and matrix elements $\rho^{\lambda}_{ij}(\sigma\tau)$ are time-independent random Gaussian numbers. The Gaussian distribution of each matrix element is specified by a mean value, $\overline{\rho^{\lambda}_{ij}}(\sigma\tau)=\delta_{ij}n_j^{\sigma\tau}$, and a variance,

$$\overline{\delta\rho^{\lambda}_{ij}(\sigma\tau)\delta\rho^{\lambda}_{j'i'}(\sigma'\tau')}=\tfrac{1}{2}\delta_{jj'}\delta_{ii'}\delta_{\tau\tau'}\delta_{\sigma\sigma'}\left[n_i^{\sigma\tau}\left(1-n_j^{\sigma\tau}\right)+n_j^{\sigma\tau}\left(1-n_i^{\sigma\tau}\right)\right], \tag{4}$$

where $n_j^{\sigma\tau}$ denotes the average occupation factor for given values of spin-isospin quantum numbers σ, τ and $\delta\rho^{\lambda}_{ij}(\sigma\tau)=\rho^{\lambda}_{ij}(\sigma\tau)-\overline{\rho^{\lambda}_{ij}}(\sigma\tau)$. $\delta_{\tau\tau'}$ and $\delta_{\sigma\sigma'}$ indicate that density matrix elements are assumed to be uncorrelated in spin-isospin space. A member of the ensemble is generated by evolving the single-particle wave functions according to the self-consistent mean-field of that member,

$$i\hbar\frac{\partial}{\partial t}\Phi_{j\sigma\tau}(\boldsymbol{r},t;\lambda)=h(\rho^{\lambda})\Phi_{j\sigma\tau}(\boldsymbol{r},t;\lambda), \tag{5}$$

where $h(\rho^{\lambda})$ is the self-consistent mean-field Hamiltonian in that event.

III. STOCHASTIC WIGNER DISTRIBUTION

To carry out projection of the SMF on a collective space, to determine transport coefficients of collective variables, and to establish a connection with the collective transport models, it is very convenient to introduce the stochastic Wigner distribution. The Wigner distribution for each event λ is defined as a partial Fourier transform of density matrix as

$$f^{\lambda}(\boldsymbol{r},\boldsymbol{p},t)=\int d^3s\exp\left(-\frac{i}{\hbar}\boldsymbol{p}\cdot\boldsymbol{s}\right)\sum_{ij\sigma\tau}\Phi^{*}_{j\sigma\tau}\left(\boldsymbol{r}+\frac{\boldsymbol{s}}{2},t;\lambda\right)\times\rho^{\lambda}_{ji}(\sigma\tau)\Phi_{i\sigma\tau}\left(\boldsymbol{r}-\frac{\boldsymbol{s}}{2},t;\lambda\right). \tag{6}$$

In this work, we focus on head-on collisions of two heavy ions and take the collision direction as the x axis. Following Ref. [19], we define the center-of-mass coordinate $R^{\lambda}_{\pm}$, the total momentum $P^{\lambda}_{\pm}$, and the mass number $A^{\lambda}_{\pm}$ of projectile-like (+) and target-like (−) fragments by introducing the separation plane. The separation plane can be conveniently defined as the plane at the position where iso-contours of projectile-like and target-like densities cross each other. We indicate the position of the separation plane, i.e., the position of the window at $x=x_0$. Illustrations of density profiles and separation plane locations are displayed at different times of the symmetric reaction $^{40}\mathrm{Ca}+{}^{40}\mathrm{Ca}$ in Fig. 1. For calculations in this figure and the rest of the article, we use the three-dimensional TDHF code developed by P. Bonche and co-workers with the SLy4d Skyrme effective force [22]. For technical details, please see Ref. [19].

It is convenient to express macroscopic variables in each event in terms of the reduced Wigner distribution $f^{\lambda}(x,p_x,t)$ according to

$$R^{\lambda}_{\pm}=\frac{1}{A^{\lambda}_{\pm}}\iint\frac{dxdp_x}{2\pi\hbar}\theta(\pm(x-x_0))xf^{\lambda}(x,p_x,t), \tag{7}$$

$$P^{\lambda}_{\pm}=\iint\frac{dxdp_x}{2\pi\hbar}\theta(\pm(x-x_0))p_xf^{\lambda}(x,p_x,t), \tag{8}$$

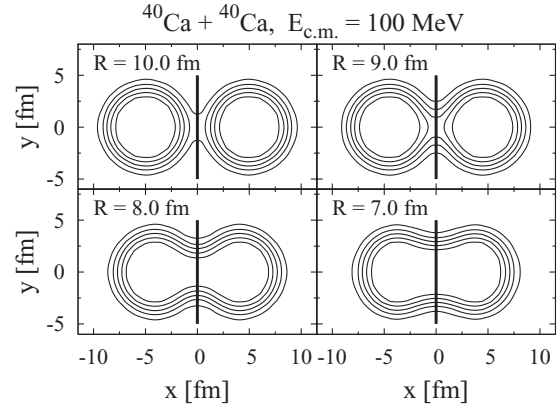

FIG. 1. Density profiles $\rho(x,y,0)$ obtained with TDHF for the $^{40}\mathrm{Ca}+{}^{40}\mathrm{Ca}$ reaction at $E_{\mathrm{c.m.}}=100$ MeV at different R. The iso-densities are plotted every 0.025 fm^{-3}. In each case, the vertical line indicates the separation plane.

and

$$A^{\lambda}_{\pm} = \iint \frac{dxdp_x}{2\pi\hbar}\theta(\pm(x-x_0))f^{\lambda}(x,p_x,t), \qquad (9)$$

where $\theta(x) = 1$ for $x \geqslant 0$ and zero elsewhere. We note that these definitions do not involve semiclassical approximations and are fully equivalent to those given in Ref. [19]. The ratio $P^{\lambda}_{\mp}/\dot{R}^{\lambda}_{\mp} = m^{\lambda}_{\mp}(R)$ determines the inertia of both sides of the window and the relative momentum is defined as

$$P^{\lambda} = \frac{m^{\lambda}_{-}P^{\lambda}_{+} - m^{\lambda}_{+}P^{\lambda}_{-}}{m^{\lambda}_{-}+m^{\lambda}_{+}} = \mu^{\lambda}(R)\dot{R}^{\lambda}, \qquad (10)$$

where $\mu^{\lambda}(R) = m^{\lambda}_{+}m^{\lambda}_{-}/(m^{\lambda}_{+}+m^{\lambda}_{-})$ and $\dot{R}^{\lambda} = \dot{R}^{\lambda}_{+} - \dot{R}^{\lambda}_{-}$ are the reduced mass and the relative velocity of projectile and target sides, respectively. The reduced Wigner distribution $f^{\lambda}(x,p_x,t)$ is obtained by integrating over the phase-space variables y, z, p_y, and p_z according to

$$f^{\lambda}(x,p_x,t) = \iiiint dydz\frac{dp_ydp_z}{(2\pi\hbar)^2}f^{\lambda}(\boldsymbol{r},\boldsymbol{p},t). \qquad (11)$$

To extract diffusion coefficients associated with collective variables, we need different-time correlation function of the reduced Wigner distribution on the window. Assuming that the amplitude of density fluctuations is small, this correlation function on the window is calculated using the semiclassical approximation in Appendix to give

$$\overline{\delta f^{\lambda}(x,p_x,t)\delta f^{\lambda}(x,p'_x,t')}|_{x=x_0} = (2\pi\hbar)\frac{m}{|p_x|}\delta(p_x-p'_x)\delta(t-t')\Lambda^{+}(x_0,p_x,t), \qquad (12)$$

where the quantity $\Lambda^{\pm}(x_0,p_x,t)$ is defined as

$$\Lambda^{\pm}(x_0,p_x,t) = \sum_{\sigma\tau}\{f^{\sigma\tau}_P(x_0,p_x,t)[1-\bar{f}^{\sigma\tau}_T(x_0,p_x,t)] \pm f^{\sigma\tau}_T(x_0,p_x,t)[1-\bar{f}^{\sigma\tau}_P(x_0,p_x,t)]\}. \qquad (13)$$

In this expression, $f^{\sigma\tau}_P(x,p_x,t)$ denotes, in the spin-isospin channel (σ,τ), the average value of the reduced Wigner function associated with wave functions originating from the projectile,

$$f^{\sigma\tau}_P(x,p_x,t) = \iint dydz\int ds_x \exp\left(-\frac{i}{\hbar}p_xs_x\right) \times \sum_{i\in P}\Phi^{*}_{i\sigma\tau}\left(x+\frac{s_x}{2},y,z,t\right)n^{\sigma\tau}_i \times \Phi_{i\sigma\tau}\left(x-\frac{s_x}{2},y,z,t\right). \qquad (14)$$

The average quantity

$$\bar{f}^{\sigma\tau}_P(x_0,p_x,t) = \frac{f^{\sigma\tau}_P(x_0,p_x,t)}{\Omega(x_0,t)} \qquad (15)$$

denotes the reduced Wigner distribution averaged over phase-space on the window, i.e., on the plane dividing projectile-like and target-like nuclei, where $\Omega(x_0,t)$ is the phase-space volume over the window. Quantities $f^{\sigma\tau}_T(x_0,p_x,t)$ and $\bar{f}^{\sigma\tau}_T(x_0,p_x,t)$ are average values of the reduced Wigner function associated with wave functions originating from the target in the spin-isospin channel (σ,τ), which are defined in a similar manner.

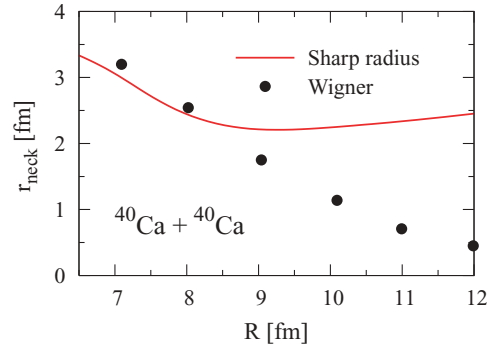

FIG. 2. (Color online) Neck radius determined for the ^{40}Ca + ^{40}Ca reaction at $E_{c.m.} = 100$ MeV by using Eq. (17) (solid line) and by imposing the condition that the reduced Wigner function $\bar{f}^{\sigma\tau}_{P/T}(x,p_x,t)$ is close to 1.0 around the average momentum (solid circles).

We approximate the phase-space volume over the window as

$$\Omega(x_0,t) = \pi r^2_{\rm neck}(x_0,t)\frac{\pi p^2_F}{(2\pi\hbar)^2}, \qquad (16)$$

where p_F stands for the Fermi momentum. In this expression $r_{\rm neck}(x_0,t)$ denotes the equivalent sharp radius of the neck, which is defined as

$$\pi r^2_{\rm neck}(x_0,t) = \frac{1}{n_0(x_0,t)}\iint dydzn(x_0,y,z,t), \qquad (17)$$

where $n(x_0,y,z,t)$ is the local nucleon density while $n_0(x_0,t)$ denotes the density at the center of the neck, i.e., $n_0(x_0,t) \equiv n(x_0,0,0,t)$. The evolution of $r_{\rm neck}$ deduced from Eq. (17) is shown by solid lines in Fig. 2 for the ^{40}Ca + ^{40}Ca reaction as a function of relative distance.

While the neck radius has rather reasonable values at small R, Eq. (17) leads to unrealistic large values for well-separated nuclei. To overcome this difficulty, we use an alternative approach by considering that $\bar{f}^{\sigma\tau}_{P/T}(x_0,p_x,t)$ should be close to 1.0 around the average value of p_x. By imposing this condition, we directly determine an approximate phase-space volume from Eq. (15). Then, we deduce $r_{\rm neck}$ at each relative distance R by inverting Eq. (16). These are indicated by solid circles in Fig. 2. We see that the second prescription not only provides a reasonable behavior for $r_{\rm neck}$ at large distances but also matches $r_{\rm neck}$ deduced by using Eq. (17) at small distances. In the calculations we use the effective neck radius determined by the second approach.

Examples of the reduced Wigner function are shown in Fig. 3 for different relative distances. Not surprisingly, the reduced Wigner function is sometimes above 1 or below 0. This is indeed expected because the full quantum Wigner transform is considered without making use of any semiclassical approximation.

IV. MOMENTUM DIFFUSION COEFFICIENT

In a recent work [19], considering simple one-dimensional macroscopic reduction of TDHF, average transport properties of relative motion in heavy-ion collisions have been

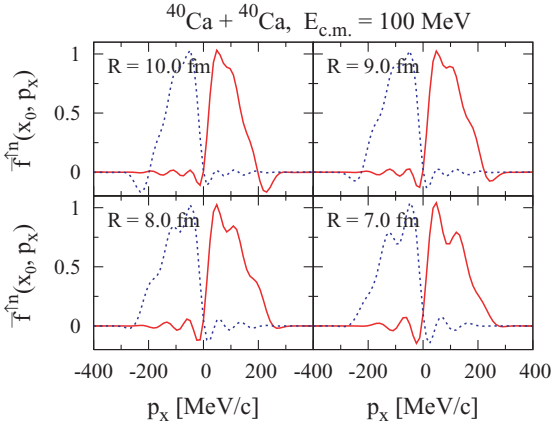

FIG. 3. (Color online) Reduced Wigner function $\bar{f}^{\uparrow n}(x_0, p_x)$ averaged over phase space on the window ($x = x_0$) for projectile-like (dotted line) and target-like (solid line) nuclei for the $^{40}Ca + ^{40}Ca$ reaction at $E_{c.m.} = 100$ MeV at different R. The Fermi momentum p_F is taken as 270 MeV/c.

investigated. The temporal evolution of the average value of relative distance $R(t) = \overline{R^\lambda(t)}$ and the average value of relative momentum $P(t) = \overline{P^\lambda(t)}$ is calculated for the average mean-field trajectory determined by the TDHF wave functions. The relative motion of colliding ions was analyzed on the basis of a simple classical equation of motion,

$$\frac{d}{dt}P = -\frac{d}{dR}U(R) - \gamma(R)\dot{R}. \tag{18}$$

Knowing the time evolution of $R(t)$ and $P(t)$, average collective properties, namely, nucleus-nucleus potential energy $U(R)$ and form factor of one-body friction coefficient $\gamma(R)$, are determined by inverting Eq. (18). In this work, we consider the same geometry of head-on collisions of heavy-ions and extend the macroscopic reduction treatment by considering the SMF approach. We analyze the relative motion by employing a Langevin equation. The Langevin equation for the relative motion has the form

$$\frac{d}{dt}P^\lambda = -\frac{d}{dR^\lambda}U(R^\lambda) - \gamma(R^\lambda)\dot{R}^\lambda + \xi_P^\lambda(t), \tag{19}$$

where $\xi_P^\lambda(t)$ is a Gaussian random force acting on the relative motion. Ignoring non-Markovian effects, the random force reduces to white noise specified by a correlation function,

$$\overline{\xi_P^\lambda(t)\xi_P^\lambda(t')} = 2\delta(t - t')D_{PP}(R). \tag{20}$$

Here $D_{PP}(R)$ denotes the momentum diffusion coefficient, which may depend on the mean value of the relative distance R.

To extract the momentum diffusion coefficient, we calculate the rate of change of the relative momentum employing the SMF equations. The rate of change of the relative momentum involves kinetic parts due to nucleon exchange between projectile and target and also involves terms arising from potential energy. In the previous investigation [21], it is observed that during evolution from the entrance channel until passing over the Coulomb barrier, the one-body dissipation mechanism is strongly correlated with nucleon exchange between projectile-like and target-like nuclei. This behavior is similar to the phenomenological nucleon exchange model and the window formula for energy dissipation [23,24]. Therefore, in the equation for the rate of change of the relative momentum, we consider only kinetic terms corresponding to momentum flow across the window, which can be conveniently expressed in terms of the reduced Wigner distribution as

$$\frac{d}{dt}P^\lambda = -\int \frac{dp_x}{2\pi\hbar}\frac{p_x^2}{m}f^\lambda(x, p_x, t)|_{x=x_0} + \text{potential terms}. \tag{21}$$

Small fluctuations of the relative momentum are connected to small amplitude fluctuations in the Wigner distribution. Ignoring contributions arising from potential terms, we have, for small fluctuations of the relative momentum,

$$\frac{d}{dt}\delta P^\lambda \approx -\int \frac{dp_x}{2\pi\hbar}\frac{p_x^2}{m}\delta f^\lambda(x, p_x, t)|_{x=x_0} = \xi_P^\lambda(t). \tag{22}$$

The right-hand side in this expression acts as a random force for generating fluctuations in the relative momentum. Because $\delta f^\lambda(x, p_x, t)$ is a Gaussian random quantity, the random force $\xi_P(t)$ is also Gaussian random, which is specified by a correlation function,

$$\overline{\xi_P^\lambda(t)\xi_P^\lambda(t')} = \iint \frac{dp_x}{2\pi\hbar}\frac{dp'_x}{2\pi\hbar}\frac{p_x^2}{m}\frac{p'^2_x}{m} \times \overline{\delta f^\lambda(x, p_x, t)\delta f^\lambda(x, p'_x, t')}|_{x=x_0}. \tag{23}$$

Using the expression for the correlation function of the reduced Wigner distribution in Eq. (12), according to Eq. (20), the momentum diffusion coefficient is given by

$$D_{PP}(t) = \int \frac{dp_x}{2\pi\hbar}\frac{|p_x|}{m}\frac{p_x^2}{2}\Lambda^+(x_0, p_x, t). \tag{24}$$

From the SMF approach, we cannot directly derive an expression for the friction coefficient $\gamma(R)$. The reason is that we cannot associate the net momentum flow across the window, which is given by the first term on the right-hand side of Eq. (21), with dissipative force acting on the relative motion. However, from the expression (24) for diffusion coefficient and from the random walk mechanism of nucleon exchange [23,24], we can infer an expression for the friction coefficient. In the expression for the diffusion coefficient, the first and second terms correspond to the nucleon flux from projectile to target and from target to projectile, respectively. Each nucleon transfer changes the relative momentum by the amount p_x and increases the dispersion of the relative momentum by the amount p_x^2. Nucleon transfer in both direction increases the dispersion of the relative momentum; therefore, the diffusion coefficient is determined by the total nucleon flux, i.e., the sum of flux from projectile to target and from target to projectile. However, dissipation is determined by the net momentum flow through the window. Hence, the resultant dissipative force can be expressed as

$$F(t) = \int \frac{dp_x}{2\pi\hbar}\frac{|p_x|}{m}p_x\Lambda^-(x_0, p_x, t). \tag{25}$$

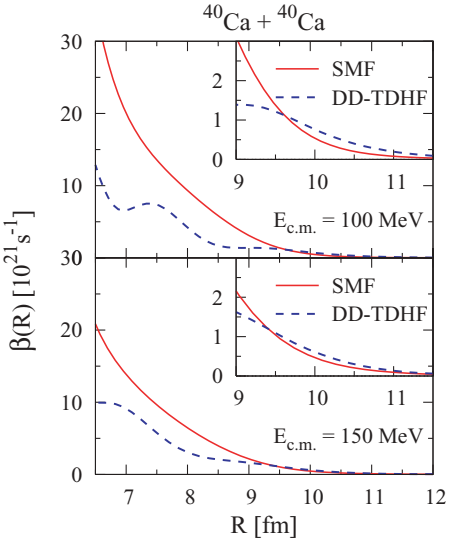

FIG. 4. (Color online) Reduced friction coefficient $\beta(R) = \gamma(R)/\mu$ as a function of R for the ^{40}Ca + ^{40}Ca reaction at $E_{\text{c.m.}} = 100$ MeV (upper panel) and at $E_{\text{c.m.}} = 150$ MeV (lower panel). For each energy, a zoom on the Coulomb barrier region is also shown in the insert.

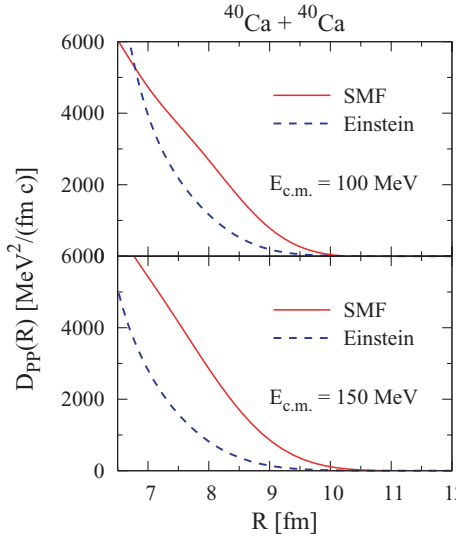

FIG. 5. (Color online) Diffusion coefficient D_{PP} obtained by SMF (solid lines) and by the Einstein relation $D^{\text{eq}}_{PP} = \gamma(R)T(t)$ (dashed lines) as a function of R for the ^{40}Ca + ^{40}Ca reaction at $E_{\text{c.m.}} = 100$ MeV (upper panel) and at $E_{\text{c.m.}} = 150$ MeV (lower panel).

Then, it is possible to deduce from TDHF simulations the momentum diffusion coefficient $D_{PP}(t) = D_{PP}(R)$ and the friction force $F(t)$ as a function of relative distance. We note that these transport coefficients correspond to the phenomenological window formula arising from the nucleon exchange mechanism [24], and they are determined in terms of the average evolution specified by the TDHF.

Rather than calculating the dissipative force, it is more instructive to calculate the friction coefficient $\gamma(R)$. For this purpose, we assume that the dissipative force is proportional to the relative velocity, i.e., $F(t) = -\gamma(R)\dot{R}$, and consider the reduced friction coefficient $\beta(R) = \gamma(R)/\mu(R)$, where $\mu(R)$ denotes inertia associated with relative motion. Solid lines in Fig. 4 show the reduced friction coefficient as a function of R for a head-on collision of ^{40}Ca + ^{40}Ca at two different center-of-mass energies. For each energy, an enlarged plot around the Coulomb barrier region is shown in the insert. In a recent work [21], we extracted the reduced friction coefficient associated with relative motion by employing a different reduction procedure, so-called Dissipative-Dynamics TDHF (DD-TDHF), which, in principle, incorporates dissipation due to both window and wall mechanisms. Dashed lines in Fig. 4 show the results of this reduction procedure. Good agreement is found between two different calculations above and close to the Coulomb barrier (∼9.8 fm). Below the Coulomb barrier, the DD-TDHF method is not reliable. However, the method based on the SMF provides a proper description of the one-body friction coefficient due to the nucleon exchange mechanism for a wide range of relative distance.

Solid lines in Fig. 5 show the momentum diffusion coefficient D_{PP}, Eq. (24), as a function of R for a head-on collision of ^{40}Ca + ^{40}Ca at two different center-of-mass energies. Similarly to the reduced friction coefficient, the magnitude of the momentum diffusion coefficient increases for decreasing relative distance. The increase of the magnitude of transport coefficients, i.e., friction and diffusion coefficients, for decreasing R is essentially due to the larger window area and the larger number of nucleon exchange between projectile-like and target-like nuclei. It is important to realize that, even though the ordinary TDHF does not contain information about density fluctuations, we can employ the average information provided by the TDHF to calculate diffusion coefficients associated with macroscopic variables. In practical applications, the momentum diffusion coefficient is usually taken as the thermal equilibrium value determined by the Einstein relation in terms of the friction coefficient and effective temperature as

$$D^{\text{eq}}_{PP}(R) = \gamma(R)T(t). \tag{26}$$

In this expression, $T(t)$ denotes the effective temperature assuming local equilibrium. It can be determined in terms of excitation energy denoted by E^* by the relation $T(t) = \sqrt{E^*(t)/a}$, where a denotes the level density parameter, taken here as $a = A/12$. We can estimate the excitation energy in terms of dissipated energy according to

$$E^*(t) = \int_0^t dt' \gamma[R(t')][\dot{R}(t')]^2. \tag{27}$$

Dashed lines in Fig. 5 show the diffusion coefficient $D^{\text{eq}}_{PP}(R)$ determined according to the Einstein relation. As seen from the figure, the Einstein relation severely underestimates the magnitude of the dynamical diffusion coefficient. The fact that the Einstein relation severely underestimates the dynamical diffusion coefficient associated with the relative motion has

already been realized in the phenomenological description of the nucleon exchange model in Ref. [24].

V. CONCLUSIONS

Recently proposed stochastic mean-field theory has incorporated both one-body dissipation and fluctuation mechanisms in a manner consistent with the quantal fluctuation-dissipation theorem of nonequilibrium statistical mechanics [15]. This is illustrated for slow collective motion by projecting the equation of motion of the SMF onto a collective space in adiabatic limit. The projection gives rise to a generalized Langevin equation for collective variables, in which mean-field dissipation and fluctuation mechanisms are connected through the quantal fluctuation-dissipation relation. Therefore, this approach provides a powerful tool for the microscopic description of low energy nuclear processes in which two-body dissipation and fluctuation mechanisms do not play important roles. The low energy processes include induced fission, heavy-ion fusion near barrier energies, and spinodal decomposition during the expansion phase of hot pieces of nuclear matter produced in heavy-ion collisions [16,25].

In this work, we carry out a different projection of the SMF approach on the relative motion in the fusion reaction by following the DD-TDHF method introduced in Ref. [19] and deduce one-body friction and one-body diffusion coefficients associated with relative motion. It is remarkable that expressions of transport coefficients for the relative motion (as well as transport coefficients for other macroscopic variables that are not mentioned in this work) have the same form as given by the phenomenological nucleon exchange model [23,24]. The phenomenological nucleon exchange model involves an important assumption, namely, when a nucleon passes through the window it instantaneously equilibrates with the new environment on the other side of the window. However, transport coefficients deduced from the SMF approach do not involve this assumption, and also they are not restricted by adiabatic or diabatic approximation. Therefore, these transport coefficients provide a microscopic basis for determining the magnitude of the actual one-body dissipation and the corresponding mean-field fluctuation mechanism. We also stress the fact that, assuming the amplitude of the density fluctuations is small, transport coefficients are calculated in terms of the average evolution determined by TDHF simulations as a function of relative distance. In the continuation of the investigations, we plan to generalize the projection procedure of the SMF approach for off-central collisions and also deduce transport coefficients for nucleon diffusion in grazing heavy-ion collisions.

ACKNOWLEDGMENTS

We thank P. Bonche for providing the 3D-TDHF code. S.A. gratefully acknowledges the CNRS for financial support and GANIL for warm hospitality extended to him during his visit. K.W. gratefully acknowledges the French Embassy in Japan for financial supports. This work is supported in part by the US DOE Grant No. DE-FG05-89ER40530.

APPENDIX: CORRELATION FUNCTION OF WIGNER DISTRIBUTION

Small amplitude fluctuations of the Wigner distribution can be expressed as

$$\delta f^{\lambda}(\boldsymbol{r},\boldsymbol{p},t)=\int d^3s\exp\left(-\frac{i}{\hbar}\boldsymbol{p}\cdot\boldsymbol{s}\right)\sum_{ij\sigma\tau}\Phi^{*}_{j\sigma\tau}\left(\boldsymbol{r}+\frac{\boldsymbol{s}}{2},t\right)\times\delta\rho^{\lambda}_{ij}(\sigma\tau)\Phi_{i\sigma\tau}\left(\boldsymbol{r}-\frac{\boldsymbol{s}}{2},t\right),\tag{A1}$$

where the single-particle wave functions are a complete set of solutions of the ordinary TDHF. The initial values of stochastic expansion coefficients $\delta\rho^{\lambda}_{ij}(\sigma\tau)$ are Gaussian random numbers as specified by Eq. (4). In principle, these coefficients evolve in time according to time-dependent RPA equations. Here, we ignore this evolution and take them as Gaussian random numbers as specified by the initial conditions. The fluctuating part of the density matrix can be separated into four groups, $\delta\rho^{\lambda}_{PP}$, $\delta\rho^{\lambda}_{TT}$, $\delta\rho^{\lambda}_{PT}$, and $\delta\rho^{\lambda}_{TP}$, which are associated with wave functions originating from projectile and target nuclei and the mixed terms. As a result, small amplitude fluctuations of the Wigner distribution separate into four parts, $\delta f^{\lambda}_{PP}(\boldsymbol{r},\boldsymbol{p},t)$, $\delta f^{\lambda}_{TT}(\boldsymbol{r},\boldsymbol{p},t)$, $\delta f^{\lambda}_{PT}(\boldsymbol{r},\boldsymbol{p},t)$, and $\delta f^{\lambda}_{TP}(\boldsymbol{r},\boldsymbol{p},t)$. We calculate the equal time correlation function of the Wigner distribution using a semiclassical approximation. First, we consider the correlation function associated with wave functions originating from the projectile. Using the Eq. (4) for the variance of the matrix elements, we deduce

$$\begin{aligned}&\overline{\delta f^{\lambda}_{PP}(\boldsymbol{r},\boldsymbol{p},t)\delta f^{\lambda}_{PP}(\boldsymbol{r}',\boldsymbol{p}',t)}\\&=\iint d^3sd^3s'\exp\left(-\frac{i}{\hbar}\boldsymbol{p}\cdot\boldsymbol{s}\right)\exp\left(-\frac{i}{\hbar}\boldsymbol{p}'\cdot\boldsymbol{s}'\right)\\&\times\sum_{ij\sigma\tau\in P}\Phi^{*}_{j\sigma\tau}\left(\boldsymbol{r}+\frac{\boldsymbol{s}}{2},t\right)\Phi_{i\sigma\tau}\left(\boldsymbol{r}-\frac{\boldsymbol{s}}{2},t\right)\\&\times\Phi^{*}_{i\sigma\tau}\left(\boldsymbol{r}'+\frac{\boldsymbol{s}'}{2},t\right)\Phi_{j\sigma\tau}\left(\boldsymbol{r}'-\frac{\boldsymbol{s}'}{2},t\right)n^{\sigma\tau}_{j}\left(1-n^{\sigma\tau}_{i}\right).\end{aligned}\tag{A2}$$

In the term that is proportional to $n^{\sigma\tau}_{j}$, we use the closure relations to find

$$\begin{aligned}&\sum_{i\in P}\Phi^{*}_{i\sigma\tau}\left(\boldsymbol{r}'+\frac{\boldsymbol{s}'}{2},t\right)\Phi_{i\sigma\tau}\left(\boldsymbol{r}-\frac{\boldsymbol{s}}{2},t\right)\\&=\delta\left(\boldsymbol{r}'-\boldsymbol{r}+\frac{\boldsymbol{s}'+\boldsymbol{s}}{2}\right).\end{aligned}\tag{A3}$$

In this expression, summation runs over a complete set of single-particle states, i.e., occupied and unoccupied states originating from the projectile. The closure relation satisfied by the complete set of states at the initial state remains valid at later times. In the second step, we introduce the Wigner distribution,

$$\begin{aligned}&\sum_{j\in P}\Phi^{*}_{j\sigma\tau}\left(\boldsymbol{r}+\frac{\boldsymbol{s}}{2},t\right)n^{\sigma\tau}_{j}\Phi_{j\sigma\tau}\left(\boldsymbol{r}'-\frac{\boldsymbol{s}'}{2},t\right)\\&=\int\frac{d^3Q}{(2\pi\hbar)^3}\exp\left[\frac{i}{\hbar}\left(\boldsymbol{r}-\boldsymbol{r}'+\frac{\boldsymbol{s}+\boldsymbol{s}'}{2}\right)\cdot\boldsymbol{Q}\right]\\&\times f^{\sigma\tau}_{P}\left(\frac{\boldsymbol{r}+\boldsymbol{r}'}{2}+\frac{\boldsymbol{s}-\boldsymbol{s}'}{4},\boldsymbol{Q},t\right),\end{aligned}\tag{A4}$$

where $f_P^{\sigma\tau}(\boldsymbol{r},\boldsymbol{p},t)$ denotes the ensemble averaged Wigner distribution associated with wave functions originating from the projectile in the spin-isospin channel (σ,τ). After making transformations, $\boldsymbol{s}=+\boldsymbol{\eta}+\boldsymbol{Y}/2$ and $\boldsymbol{s}'=-\boldsymbol{\eta}+\boldsymbol{Y}/2$, the term that is proportional to the occupation factor $n_j^{\sigma\tau}$ in the right-hand side of Eq. (A2) becomes

$$\sum_{\sigma\tau}\iiint d^3Y d^3\eta \exp\left[-\frac{i}{\hbar}\left(\boldsymbol{Y}\cdot\frac{\boldsymbol{p}+\boldsymbol{p}'}{2}\right)\right] \times \exp\left[-\frac{i}{\hbar}\boldsymbol{\eta}\cdot(\boldsymbol{p}-\boldsymbol{p}')\right]\frac{d^3Q}{(2\pi\hbar)^3}\exp\left[\frac{i}{\hbar}\boldsymbol{Y}\cdot\boldsymbol{Q}\right] \times f_P^{\sigma\tau}\left(\boldsymbol{r}-\frac{\boldsymbol{Y}}{4}+\frac{\boldsymbol{\eta}}{2},\boldsymbol{Q},t\right)\delta\left(\boldsymbol{r}'-\boldsymbol{r}+\frac{\boldsymbol{Y}}{2}\right). \quad \text{(A5)}$$

Assuming that the Wigner distribution is a smooth function of $\boldsymbol{r}$, $f_P^{\sigma\tau}(\boldsymbol{r}-\frac{\boldsymbol{Y}}{4}+\frac{\boldsymbol{\eta}}{2},\boldsymbol{Q},t)\approx f_P^{\sigma\tau}(\boldsymbol{r},\boldsymbol{Q},t)$ and $\delta(\boldsymbol{r}'-\boldsymbol{r}+\frac{\boldsymbol{Y}}{2})\approx\delta(\boldsymbol{r}-\boldsymbol{r}')$, we can carry out the integrations over $\boldsymbol{\eta}$ and $\boldsymbol{Y}$ to obtain $(2\pi\hbar)^3\delta(\boldsymbol{p}-\boldsymbol{p}')$ and $(2\pi\hbar)^3\delta(\boldsymbol{p}-\boldsymbol{Q})$, respectively. As a result, the term (A5) becomes

$$\text{(A5)}=(2\pi\hbar)^3\delta(\boldsymbol{p}-\boldsymbol{p}')\delta(\boldsymbol{r}-\boldsymbol{r}')\sum_{\sigma\tau}f_P^{\sigma\tau}(\boldsymbol{r},\boldsymbol{p},t). \quad \text{(A6)}$$

For the term proportional to $n_i^{\sigma\tau}n_j^{\sigma\tau}$ in Eq. (A2), again we introduce the Wigner distribution for the factor involving the index j,

$$\sum_{j\in P}\Phi^*_{j\sigma\tau}\left(\boldsymbol{r}+\frac{\boldsymbol{s}}{2}\right)n_j^{\sigma\tau}\Phi_{j\sigma\tau}\left(\boldsymbol{r}'-\frac{\boldsymbol{s}'}{2}\right) = \int\frac{d^3Q_1}{(2\pi\hbar)^3}\exp\left[\frac{i}{\hbar}\left(\boldsymbol{r}-\boldsymbol{r}'+\frac{\boldsymbol{s}+\boldsymbol{s}'}{2}\right)\cdot\boldsymbol{Q}_1\right] \times f_P^{\sigma\tau}\left(\frac{\boldsymbol{r}+\boldsymbol{r}'}{2}+\frac{\boldsymbol{s}-\boldsymbol{s}'}{4},\boldsymbol{Q}_1,t\right), \quad \text{(A7)}$$

and for the one involving the index i,

$$\sum_{i\in P}\Phi^*_{i\sigma\tau}\left(\boldsymbol{r}'+\frac{\boldsymbol{s}'}{2}\right)n_i^{\sigma\tau}\Phi_{i\sigma\tau}\left(\boldsymbol{r}-\frac{\boldsymbol{s}}{2}\right) = \int\frac{d^3Q_2}{(2\pi\hbar)^3}\exp\left[\frac{i}{\hbar}\left(\boldsymbol{r}'-\boldsymbol{r}+\frac{\boldsymbol{s}+\boldsymbol{s}'}{2}\right)\cdot\boldsymbol{Q}_2\right] \times f_P^{\sigma\tau}\left(\frac{\boldsymbol{r}+\boldsymbol{r}'}{2}+\frac{\boldsymbol{s}'-\boldsymbol{s}}{4},\boldsymbol{Q}_2,t\right). \quad \text{(A8)}$$

Making the same transformations, $\boldsymbol{s}=+\boldsymbol{\eta}+\boldsymbol{Y}/2$ and $\boldsymbol{s}'=-\boldsymbol{\eta}+\boldsymbol{Y}/2$, the term that is proportional to $n_i^{\sigma\tau}n_j^{\sigma\tau}$ in the right-hand side of Eq. (A2) becomes

$$\sum_{\sigma\tau}\iiint d^3Y d^3\eta\exp\left[-\frac{i}{\hbar}\left(\boldsymbol{Y}\cdot\frac{\boldsymbol{p}+\boldsymbol{p}'}{2}\right)\right] \times\exp\left[-\frac{i}{\hbar}\boldsymbol{\eta}\cdot(\boldsymbol{p}-\boldsymbol{p}')\right]\frac{d^3Q_1}{(2\pi\hbar)^3}\frac{d^3Q_2}{(2\pi\hbar)^3} \times\exp\left[\frac{i}{\hbar}\left(\boldsymbol{r}-\boldsymbol{r}'+\frac{\boldsymbol{Y}}{2}\right)\cdot\boldsymbol{Q}_1\right] \times\exp\left[\frac{i}{\hbar}\left(\boldsymbol{r}'-\boldsymbol{r}+\frac{\boldsymbol{Y}}{2}\right)\cdot\boldsymbol{Q}_2\right] \times f_P^{\sigma\tau}\left(\frac{\boldsymbol{r}+\boldsymbol{r}'}{2}+\frac{\boldsymbol{\eta}}{2},\boldsymbol{Q}_1,t\right) \times f_P^{\sigma\tau}\left(\frac{\boldsymbol{r}+\boldsymbol{r}'}{2}-\frac{\boldsymbol{\eta}}{2},\boldsymbol{Q}_2,t\right). \quad \text{(A9)}$$

We introduce another change of variables $\boldsymbol{Q}_1=\boldsymbol{Q}+\boldsymbol{q}/2$ and $\boldsymbol{Q}_2=\boldsymbol{Q}-\boldsymbol{q}/2$, and again assume that the Wigner distribution has a smooth function of $\boldsymbol{r}$ and ignore $\boldsymbol{\eta}$ dependence. Then, integrations over $\boldsymbol{\eta}$, $\boldsymbol{q}$ and $\boldsymbol{Y}$ give $(2\pi\hbar)^3\delta(\boldsymbol{p}-\boldsymbol{p}')$, $(2\pi\hbar)^3\delta(\boldsymbol{r}-\boldsymbol{r}')$ with $\boldsymbol{Q}_1\approx\boldsymbol{Q}_2=\boldsymbol{Q}$ and $(2\pi\hbar)^3\delta(\boldsymbol{p}-\boldsymbol{Q})$, respectively. As a result, the term (A9) becomes

$$\text{(A9)}=(2\pi\hbar)^3\delta(\boldsymbol{p}-\boldsymbol{p}')\delta(\boldsymbol{r}-\boldsymbol{r}') \times\sum_{\sigma\tau}f_P^{\sigma\tau}(\boldsymbol{r},\boldsymbol{p},t)f_P^{\sigma\tau}(\boldsymbol{r},\boldsymbol{p},t). \quad \text{(A10)}$$

Combining together, the equal time correlation function (A2) of the Wigner distribution associated with wave functions originating from projectile becomes

$$\overline{\delta f_{PP}^{\lambda}(\boldsymbol{r},\boldsymbol{p},t)\delta f_{PP}^{\lambda}(\boldsymbol{r}',\boldsymbol{p}',t)} =(2\pi\hbar)^3\delta(\boldsymbol{p}-\boldsymbol{p}')\delta(\boldsymbol{r}-\boldsymbol{r}') \times\sum_{\sigma\tau}f_P^{\sigma\tau}(\boldsymbol{r},\boldsymbol{p},t)\left[1-f_P^{\sigma\tau}(\boldsymbol{r},\boldsymbol{p},t)\right]. \quad \text{(A11)}$$

In a similar manner, we can calculate the correlation function of the Wigner distribution associated with wave functions originating from the target and from the mixed configuration,

$$\overline{\delta f_{TT}^{\lambda}(\boldsymbol{r},\boldsymbol{p},t)\delta f_{TT}^{\lambda}(\boldsymbol{r}',\boldsymbol{p}',t)} =(2\pi\hbar)^3\delta(\boldsymbol{p}-\boldsymbol{p}')\delta(\boldsymbol{r}-\boldsymbol{r}') \times\sum_{\sigma\tau}f_T^{\sigma\tau}(\boldsymbol{r},\boldsymbol{p},t)\left[1-f_T^{\sigma\tau}(\boldsymbol{r},\boldsymbol{p},t)\right] \quad \text{(A12)}$$

and

$$\overline{\delta f_{PT}^{\lambda}(\boldsymbol{r},\boldsymbol{p},t)\delta f_{PT}^{\lambda}(\boldsymbol{r}',\boldsymbol{p}',t)} =(2\pi\hbar)^3\delta(\boldsymbol{p}-\boldsymbol{p}')\delta(\boldsymbol{r}-\boldsymbol{r}')\Lambda^{+}(\boldsymbol{r},\boldsymbol{p},t), \quad \text{(A13)}$$

where

$$\Lambda^{+}(\boldsymbol{r},\boldsymbol{p},t)=\sum_{\sigma\tau}\left\{f_P^{\sigma\tau}(\boldsymbol{r},\boldsymbol{p},t)\left[1-f_T^{\sigma\tau}(\boldsymbol{r},\boldsymbol{p},t)\right] +f_T^{\sigma\tau}(\boldsymbol{r},\boldsymbol{p},t)\left[1-f_P^{\sigma\tau}(\boldsymbol{r},\boldsymbol{p},t)\right]\right\}. \quad \text{(A14)}$$

The total correlation function of the Wigner distribution is the sum of Eqs. (A11), (A12), and (A13). In the mean-field description, the subspaces of wave functions originating from projectile and target nuclei behave like pure states. Therefore, contributions of correlations coming from direct terms involving $f_P^{\sigma\tau}(\boldsymbol{r},\boldsymbol{p},t)[1-f_P^{\sigma\tau}(\boldsymbol{r},\boldsymbol{p},t)]$ and $f_T^{\sigma\tau}(\boldsymbol{r},\boldsymbol{p},t)[1-f_T^{\sigma\tau}(\boldsymbol{r},\boldsymbol{p},t)]$ are expected to be small. Hence, we can approximately express the total correlation function of the Wigner distribution as

$$\overline{\delta f^{\lambda}(\boldsymbol{r},\boldsymbol{p},t)\delta f^{\lambda}(\boldsymbol{r}',\boldsymbol{p}',t)} \approx(2\pi\hbar)^3\delta(\boldsymbol{p}-\boldsymbol{p}')\delta(\boldsymbol{r}-\boldsymbol{r}')\Lambda^{+}(\boldsymbol{r},\boldsymbol{p},t). \quad \text{(A15)}$$

We also want to calculate different time correlation functions of the Wigner distribution. Assuming that the correlation function has a short correlation time, i.e., much shorter than that of the mean-free path, different time correlation functions

can be deduced by observing that, in short time intervals of order of correlation time $|t - t'| \leqslant \tau_{\rm corr}$, the Wigner distribution may be approximated as a free propagation, $\delta f(\boldsymbol{r}, \boldsymbol{p}, t + \tau) \approx \delta f(\boldsymbol{r} - \tau \boldsymbol{p}/m, \boldsymbol{p}, t)$. As a result, different time correlation functions can be expressed as

$$\overline{\delta f^{\lambda}(\boldsymbol{r}, \boldsymbol{p}, t)\delta f^{\lambda}(\boldsymbol{r}', \boldsymbol{p}', t')} = (2\pi\hbar)^3\delta(\boldsymbol{p} - \boldsymbol{p}')\delta[\boldsymbol{r} - \boldsymbol{r}' - (t - t')\boldsymbol{p}/m]\Lambda^{+}(\boldsymbol{r}, \boldsymbol{p}, t). \tag{A16}$$

To deduce the correlation function on the window $x = x' = x_0$, we notice that

$$\delta[\boldsymbol{r} - \boldsymbol{r}' - (t - t')\boldsymbol{p}/m] \to \frac{m}{|p_x|}\delta(t - t')\delta(y - y')\delta(z - z'). \tag{A17}$$

In determining transport coefficients, we need to carry out integration over window variables, y, z, p_y, p_z, of the product of Wigner distributions. Because construction of three-dimensional Wigner functions in terms of TDHF wave functions requires a large numerical effort, we introduce the following approximation for the phase-space integration over the window,

$$\iint dydz\frac{dp_y dp_z}{(2\pi\hbar)^2} f_P^{\sigma\tau}(\boldsymbol{r}, \boldsymbol{p}, t) f_T^{\sigma\tau}(\boldsymbol{r}, \boldsymbol{p}, t) \approx \frac{1}{\Omega(x, t)} f_P^{\sigma\tau}(x, p_x, t) f_T^{\sigma\tau}(x, p_x, t). \tag{A18}$$

Here $\Omega(x, t)$ denotes the phase-space volume on the window. As a result, the correlation function on the window can be expressed in terms of the reduced Wigner distributions along the x axis given by Eq. (12).

[1] P. Ring and P. Schuck, *The Nuclear Many-Body Problem* (Springer, New York, 1980).
[2] K. Goeke and P.-G. Reinhard, *Time-Dependent Hartree-Fock and Beyond* (Bad Honnef, Germany, 1982).
[3] K. T. D. Davis, K. R. S. Devi, S. E. Koonin, and M. Strayer, in *Treatise in Heavy-Ion Science*, edited by D. A. Bromley (Plenum, New York, 1984), Vol. 4.
[4] C. Simenel, B. Avez, and D. Lacroix, in Lecture notes of the International Joliot-Curie School, Maubuisson, September 17–22, 2007, arXiv:0806.2714.
[5] S. E. Koonin, Prog. Part. Nucl. Phys. **4**, 283 (1980).
[6] J. W. Negele, Rev. Mod. Phys. **54**, 913 (1982).
[7] C. W. Gardiner, *Quantum Noise* (Springer-Verlag, Berlin, 1991).
[8] U. Weiss, *Quantum Dissipative Systems* (World Scientific, Singapore, 1999).
[9] S. Ayik and C. Gregoire, Phys. Lett. **B212**, 269 (1988); Nucl. Phys. **A513**, 187 (1990).
[10] J. Randrup and B. Remaud, Nucl. Phys. **A514**, 339 (1990).
[11] Y. Abe, S. Ayik, P.-G. Reinhard, and E. Suraud, Phys. Rep. **275**, 49 (1996).
[12] D. Lacroix, S. Ayik, and Ph. Chomaz, Prog. Part. Nucl. Phys. **52**, 497 (2004).
[13] C. H. Dasso, in *Proceedings of the Second La Rapida Summer School on Nuclear Physics*, edited by M. Lozano and G. Madurga (World Scientific, Singapore, 1985).
[14] C. H. Dasso and R. Donangelo, Phys. Lett. **B276**, 1 (1992).
[15] S. Ayik, Phys. Lett. **B658**, 174 (2008).
[16] S. Ayik, N. Er, O. Yilmaz, and A. Gokalp, Nucl. Phys. **A812**, 44 (2008).
[17] R. Balian and M. Veneroni, Phys. Lett. **B136**, 301 (1984).
[18] H. Mori, Prog. Theor. Phys. **33**, 423 (1965).
[19] K. Washiyama and D. Lacroix, Phys. Rev. C **78**, 024610 (2008).
[20] A. S. Umar and V. E. Oberacker, Phys. Rev. C **74**, 061601(R) (2006); **76**, 014614 (2007).
[21] K. Washiyama, D. Lacroix, and S. Ayik, Phys. Rev. C **79**, 024609 (2009).
[22] K.-H. Kim, T. Otsuka, and P. Bonche, J. Phys. G: Nucl. Part. Phys. **23**, 1267 (1997).
[23] J. Randrup and W. J. Swiatecki, Ann. Phys. (NY) **125**, 193 (1980); Nucl. Phys. **A429**, 105 (1984).
[24] H. Feldmeier, Rep. Prog. Phys. **50**, 915 (1987).
[25] M. Colonna, Ph. Chomaz, and S. Ayik, Phys. Rev. Lett. **88**, 122701 (2002).